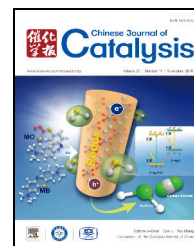


available at www.sciencedirect.comjournal homepage: www.elsevier.com/locate/chnjc

Article

Alcohol-treated SiO₂ as the support of Ir-Re/SiO₂ catalysts for glycerol hydrogenolysis

Wenting Luo^{a,c}, Yuan Lyu^{a,#}, Leifeng Gong^a, Hong Du^{a,c}, Miao Jiang^{a,c}, Yunjie Ding^{a,b,*}^a Dalian National Laboratory for Clean Energy, Dalian Institute of Chemical Physics, Chinese Academy of Sciences, Dalian 116023, Liaoning, China^b State Key Laboratory for Catalysis, Dalian Institute of Chemical Physics, Chinese Academy of Sciences, Dalian 116023, Liaoning, China^c University of Chinese Academy of Sciences, Beijing 100049, China

ARTICLE INFO

Article history:

Received 25 July 2016

Accepted 30 August 2016

Published 5 November 2016

Keywords:

Glycerol hydrolysis

1,3-Propanediol

Iridium

Rhenium

Alcohol pretreatment

ABSTRACT

The surface of SiO₂ support was pretreated by C1–C4 normal alcohols before the impregnation of iridium and rhenium precursors. These catalysts were applied in high concentration glycerol aqueous solution hydrogenolysis. The catalysts prepared from the pretreated supports exhibited high catalytic activity because of the formation of more active sites from a high dispersion of iridium oxide and rhenium oxide. The catalysts with the support pretreated by 1-propanol showed the highest glycerol conversion of 59.5%. The supports and catalysts were characterized by FT-IR, nitrogen adsorption, TPR, XRD, TEM, H₂-chemisorption and NH₃-TPD.

© 2016, Dalian Institute of Chemical Physics, Chinese Academy of Sciences.

Published by Elsevier B.V. All rights reserved.

1. Introduction

As a major byproduct of biodiesel synthesis, crude glycerol will accumulate to lead to a big environmental problem, so the conversion of crude glycerol to valuable products becomes necessary [1,2]. An appreciable number of commodity chemicals and chemical intermediates can be obtained from glycerol by catalytic processes including oxidation, dehydration, hydrogenolysis, pyrolysis, polymerization, esterification, steam reforming, acetalization, transesterification, and etherification [3,4]. Among these processes, glycerol hydrogenolysis is very promising. Hydrogenolysis of glycerol gives products such as 1,3-propanediol, 1,2-propanediol, ethylene glycol, 1-propanol and 2-propanol. 1,3-propanediol is the monomer of polytrimethylene terephthalate (PTT) and is also applied in the production of cosmetics, foods, lubricants and medicines, so

1,3-propanediol has great economic value. Therefore, the hydrogenolysis of glycerol to 1,3-propanediol have recently received more attention [5].

Many catalysts for glycerol hydrogenolysis were recently studied. Re promoted this reaction when added to noble metals such as Pt, Rh, Pd, Ir and Ru [6–14]. Rhenium oxide will form Re-OH species when it is exposed to steam [15]. Re-OH interacts with the OH groups of glycerol to form 2,3-dihydroxypropaneoxide, and then hydrogen species will activate the secondary carbon of the 2,3-dihydroxypropaneoxide to cleave the C–O bond. Then hydrolysis occurs to release the product [8,16–19].

The dispersion of the active metal component has a great influence on the catalytic performance [20,21]. The metal dispersion can be improved by using SiO₂ support pretreated with monohydric alcohols [22], organic acid [23,24], dihydric alcohol [25–27], alkali [28] and silane [24]. These solvents change

* Corresponding author. Tel/Fax: +86-411-84379143; E-mail: dylj@dicp.ac.cn# Corresponding author. Tel/Fax: +86-411-84379143; E-mail: luyuan@dicp.ac.cn

This work was supported by the National Natural Science Foundation of China (21403217).

DOI: 10.1016/S1872-2067(16)62517-2 | <http://www.sciencedirect.com/science/journal/18722067> | Chin. J. Catal., Vol. 37, No. 11, November 2016

the surface property of SiO₂ by decreasing surface hydroxyl groups, adding organic groups and changing the hydrophobic properties, which lead to better dispersion of the active metal particles.

In the present study, we prepared Ir-Re/SiO₂ catalysts with SiO₂ pretreated by C1–C4 normal alcohols. The catalytic performances of the alcohol-pretreated SiO₂ supported catalysts for glycerol hydrogenolysis to 1,3-propanediol was tested and compared with the catalyst prepared using non-pretreated SiO₂. Support pretreatment increased the dispersion of iridium. The carbon chain length of the alcohol used for the pretreatment influenced the surface properties of the support and has an impact on the dispersion of Ir species.

2. Experimental

2.1. Catalyst preparation

Silica gel (Qingdao Haiyang Chemicals Co.) was dried at 383 K for 4 h, and then used as the support which is denoted as S here. For the support pretreatment, the silica gel (2 g) was treated with 5 mL each of the C1 to C4 normal alcohols by impregnation. The resultant silica gel was dried at 383 K for 4 h after preliminary drying under ambient conditions. These were denoted as S-C_n ($n=1-4$, n is the carbon number of alcohol).

Ir-Re/S-C_n ($n=1-4$) was prepared by co-impregnation with aqueous solutions of H₂IrCl₆ (Tianjin Fengchuan Chemical Reagent Co., Ltd) and NH₄ReO₄ (Zhuzhou Jinlai Industry Co., Ltd) simultaneously of the support pretreated with alcohol. This was followed by drying at 393 K for 12 h and calcining at 773 K for 3 h. Ir-Re/S was prepared by using non-treated silica. The other procedures were the same as that of the Ir-Re/S-C_n ($n=1-4$) catalysts. Both of the contents of iridium and rhenium were 2 wt%. All chemicals used were analytical reagent.

2.2. Characterization

Nitrogen adsorption isotherms of the catalyst samples were measured at 77 K with an Autosorb-iQ adsorption analyzer (Quantachrome). The specific surface area of the samples was calculated by the Brunauer-Emmett-Teller (BET) method. The total pore volume of the samples was calculated from the amount adsorbed at a relative pressure $p/p_0 = 0.995$.

Fourier transform infrared (FT-IR) spectra were obtained using a Thermo Scientific Nicolet iS50 FT-IR spectrometer equipped with a DTGS detector. The sample was heated to 473 K for 1 h in vacuum. Spectra were collected in the range of 2400–4000 cm⁻¹ with 4 cm⁻¹ resolution.

Powder X-ray diffraction (XRD) analysis was performed on an X'pert PRO/PANalytical diffractometer using Cu K_α radiation and operated at 40 kV and 40 mA. The XRD patterns were recorded for 2θ values from 10° to 80°. The scanning rate was 14°/min. TEM measurements were carried out using a JEM-2100 microscope operated at an accelerating voltage of 200 kV. The spent catalyst was suspended in ethanol and placed onto a carbon film supported over a copper grid.

Temperature programmed reduction (TPR) was performed

on an AMI-300 catalyst characterization system. Approximately 100 mg of the sample was placed in a quartz reactor and heated to 403 K to eliminate moisture. Then the sample was reduced in a 10% H₂/Ar flow at 40 mL/min from 323 to 773 K at a heating rate of 10 K/min. H₂-TPD was carried out on an AMI-300 catalyst characterization system. 100 mg of catalyst was heated to 773 K for 1 h in an argon flow. Then the sample was reduced in a 10% H₂/Ar flow at 443 K for 2 h, and cooled down to 303 K after holding for 1 h. After that, the hydrogen in the system was replaced by argon to conduct the TPD experiment. The heating rate was kept at 10 K/min, and the flow rate of argon was 30 mL/min. H₂ chemisorption was performed on an AMI-300 catalyst characterization system. About 100 mg of the catalyst sample was reduced in a flow of 10% H₂/Ar at 443 K for 2 h, then purged by argon at the same temperature for 0.5 h, and finally cooled down to 313 K. Uptake of H₂ was measured by injecting 10% H₂/Ar into the argon carrier gas in a pulsed mode. Temperature programmed desorption of ammonia (NH₃-TPD) was carried out on an AMI-300 catalyst characterization system. A 100 mg sample was used. Prior to each measurement, a sample was pretreated in an argon flow at 873 K for 0.5 h. After cooling to 373 K in a continuous flow of argon, the sample adsorbed NH₃ using the static adsorption method until saturation. Then the sample was heated from 373 to 873 K with a ramp of 10 K/min in a helium flow of 30 mL/min and the desorbed NH₃ was monitored simultaneously with TCD.

The acidity of the catalyst was analyzed by FT-IR of adsorbed pyridine using a Thermo Scientific Nicolet iS50 FT-IR spectrometer equipped with a DTGS detector. 10 mg of a sample was pressed into a self-supporting wafer followed by evacuation at 773 K for 1 h. After cooling down to room temperature, the background spectrum was recorded. The sample was exposed to pyridine for 5 min. After that the catalyst was heated at a linear rate of 10 K/min to 323, 523 and 623 K, respectively, and kept for 0.5 h at each temperature under vacuum conditions (10 mPa). In situ FT-IR spectra of CO adsorption were recorded a Thermo Scientific Nicolet iS50 FT-IR spectrometer equipped with a DTGS detector. Before characterization, the sample (about 10 mg spent catalyst) was compressed into a self-supporting disc and reduced in a H₂ flow of 40 mL/min at 523K. The sample was heated in vacuum for 1 h at 773 K, and then cooled down to room temperature, at which point a background spectrum was acquired. The sample was then exposed to CO flow. After 30 min, the cell was evacuated to remove physisorbed and gas phase CO. Then the spectra of CO chemisorption on the sample were taken. All the gases used in characterization were analytical reagent from Guangming Research & Design Institute of Chemical Industry.

2.3. Catalytic activity measurements

The glycerol hydrogenolysis reaction was performed in a trickle bed reactor (9 mm i.d.) using 1.5 g catalyst. The hydrogen flow was 40 mL/min which corresponded to a space velocity of 1600 mL/(h·g). The glycerol aqueous flow was 0.65 mL/h which corresponded to a space velocity of 0.44 mL/(h·g). Before reaction, the catalyst was reduced at 443 K in H₂ flow of 40

mL/min at atmosphere pressure. The reaction was conducted at 403 K and 8 MPa. The gaseous products from the effluent were analyzed online using an Agilent GC-7890 chromatograph. The liquid phase products were quantified by an internal standard method, and the internal standard was *n*-butyl alcohol. Then, the liquid phase products were esterified by acetic anhydride catalyzed by pyridine (Tianjin Kemiou Chemical Reagent Co. Ltd) and heated to 328 K for 1.5 h. The volume ratio of acetic anhydride and pyridine is 2:1. The samples were quantified on a gas chromatograph (Agilent 7890) fitted with a flame ionization detector and a HP-5 capillary column. The conversion of glycerol and the selectivity to the products were calculated by the following equations:

Conversion of glycerol (%) = (moles of glycerol initially added – moles of glycerol that remained) / moles of glycerol initially added × 100

Selectivity (%) = C mole of specific product / sum of C mole of glycerol consumed × 100

The removal selectivity of primary (or secondary) hydroxyl group (%) (S_{1-OH} or S_{2-OH}) = sum of removal primary or secondary hydroxyl group / sum of removal hydroxyl group × 100

The yield of removal secondary hydroxyl group (Y_{2-OH} , %) = Conversion of glycerol × removal selectivity of secondary hydroxyl group

3. Results and discussion

3.1. Characterization of the support pretreated with different alcohols

As shown in Fig. 1, the broad band between 3100 and 3700 cm^{-1} was attributed to the hydrogen-bonded Si–OH stretching vibrations. The peak centered at 3743 cm^{-1} was attributed to the isolated Si–OH stretching vibrations. The absorption bands at 2800 to 3000 cm^{-1} were assigned to the C–H stretching vibrations of surface alkoxy groups [22,29–32]. Obvious absorption bands corresponding to alkoxy groups appeared on the pretreated SiO_2 , which suggested that alcohol molecules were grafted onto the silica surface by reacting with the Si–OH after the SiO_2 pretreatment. In addition, the ratio of isolated to adja-

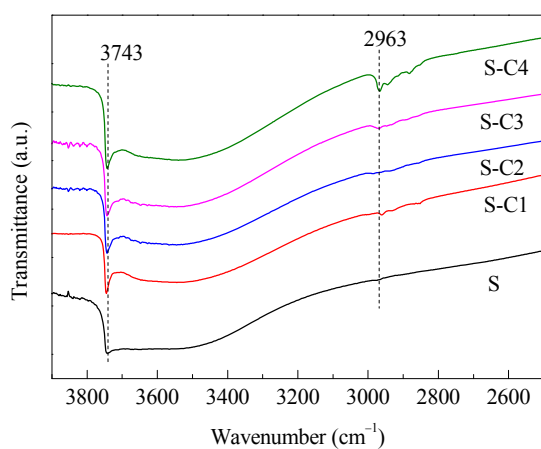


Fig. 1. FT-IR spectra of SiO_2 and alcohol-pretreated SiO_2 supported catalysts.

Table 1
Specific surface area and pore volume of untreated and pretreated SiO_2 .

Sample	S_{BET} (m^2/g)	Pore volume (cm^3/g)	Mass loss (%) ^a	Mole of alcohol molecule (0.1 mmol/g)
S	426.8	1.24	—	—
S-C1	257.4	0.98	—	—
S-C2	282.2	1.04	1.2	2.6
S-C3	305.8	1.14	1.5	2.5
S-C4	291.2	1.08	0.9	1.2

^aResults from thermogravimetric analysis.

cent Si–OH increased for the pretreated SiO_2 .

The specific surface area and pore volume obtained from the nitrogen adsorption isotherms are shown in Table 1. The specific surface area and pore volume of the pretreated SiO_2 were less than those of the untreated one. This may result from the grafting of alkoxy groups in the pores of the SiO_2 support. With the increase of carbon number in the alcohol molecules, both the specific surface area and pore volume increased first and then decreased a little. The maximum was obtained for the S-C3 support. The reason why the specific surface area and pore volume of S-C3 and S-C4 were larger than those of the smaller alcohols may be due to that the number of grafted alcohol molecules of S-C1 and S-C2 were larger, which was consistent with the thermogravimetric analysis results shown in Table 1. When the support was treated with C2–C4 alcohols, the moles of alcohol molecule adsorbed decreased as the carbon number increased.

3.2. Characterization of the alcohol-pretreated SiO_2 supported catalysts

The TPR profiles of the catalysts are shown in Fig. 2. In the case of Re/S, a single reduction peak at 583 K was observed. In the TPR profile of Ir/S, the reduction peak at 493 K can be assigned to the reduction of iridium. Compared with the TPR profiles of Re/S and Ir/S, obvious shifts of the reduction temperature towards lower temperature were observed on the Ir-Re/S catalysts. It is known that the addition of Re improved the dispersion of Ir species [8]. Smaller IrO_2 particles on the Ir-Re catalysts are more easily reduced, and then by the hy-

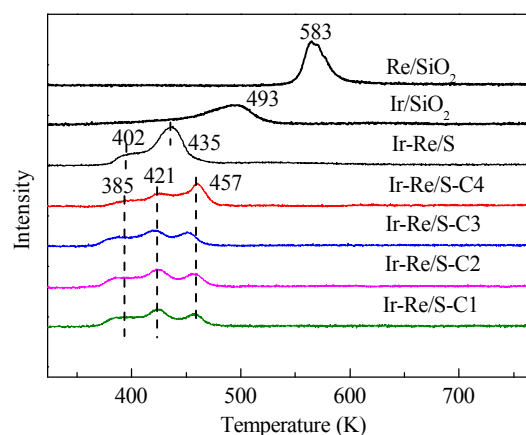


Fig. 2. H_2 -TPR profiles of alcohol-pretreated SiO_2 supported catalysts.

drogen spillover mechanism, migration of the dissociated hydrogen from IrO₂ to Re oxide resulted in the improvement of the reduction of Re oxide, so the reduction temperature shifted toward lower temperature. The TPR profile of Ir-Re/S showed two broad peaks, but the reduction profile of the alcohol-pretreated SiO₂ supported catalysts was characterized by three reduction peaks. The reduction started at lower temperature on the alcohol-pretreated SiO₂ supported catalysts, which suggested that smaller Ir species particles were formed on these catalysts. The low temperature reduction peak was observed at 385 K on the alcohol-pretreated SiO₂ supported catalysts and 402 K on Ir-Re/S, which was assigned to the reduction of Ir species. The subsequent reduction peak at 421 or 435 K was attributed to the co-reduction of Ir and Re oxide species. The high temperature peak that only existed on the pretreated catalysts at 457 K may be due to the reduction of IrO₂ or Re oxide species with a stronger interaction with the support [33,34]. If all Ir⁴⁺ was supposed to be reduced to Ir⁰, the valence of the Re species can be calculated by the H₂ consumption, which is summarized in Table 2. The Re valence of the alcohol-pretreated SiO₂ supported catalysts and untreated one were approximately 4.5, but that on Re/S was measured to be 2.7. This indicated that the Re species has an interaction with Ir species or the support in the Ir-Re catalysts.

Fig. 3 shows the XRD patterns of the fresh catalysts. The diffraction peak at $2\theta = 21.4^\circ$ was attributed to amorphous silica gel. The diffraction peaks at $26.7^\circ(110)$, $34.2^\circ(101)$ and $53.1^\circ(211)$ can be readily indexed to IrO₂ (PDF 01-088-0288). As shown in Fig. 4, a diffused diffraction peak at $2\theta = 40.5^\circ$ was observed on the spent catalysts, which corresponded to metal-

Table 2
TPR results of different samples.

Catalyst	H ₂ consumption ($\mu\text{mol/g}$)	Re valence
Ir-Re/S	337.2	4.6
Ir-Re/S-C1	333.2	4.6
Ir-Re/S-C2	338.1	4.6
Ir-Re/S-C3	346.8	4.4
Ir-Re/S-C4	338.3	4.5
Re/S	228.1	2.7

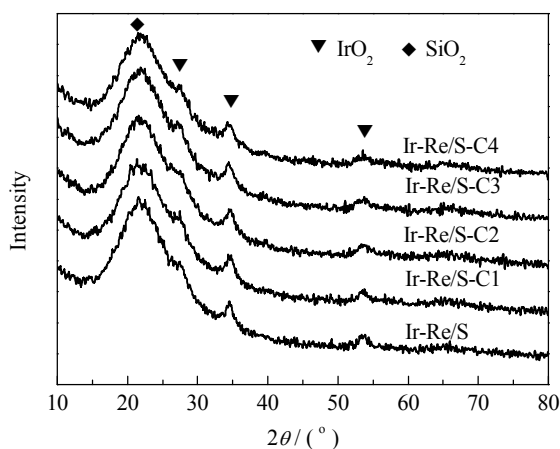


Fig. 3. XRD patterns of alcohol-pretreated SiO₂ supported catalysts before reaction.

lic iridium (PDF 01-087-0715). For both the fresh or spent catalysts, a peak due to Re species was not detected, indicating that the Re species was highly dispersed.

Fig. 5 displays the TEM images of the spent catalysts. The Ir species and Re species were hard to distinguish by the lattice fringes. But these visible particles were thought to be Ir species because the Re species particles were so small that they would be difficult to observe according to the results of XRD [8]. The Ir average particle size calculated statistically by TEM are shown in Table 3. It was found that the pretreated supports benefited the dispersion of Ir and all of the alcohol-pretreated SiO₂ supported catalysts showed a smaller Ir average particle size. Ir-Re/S-C3 presented the smallest Ir particles. The TEM results were consistent with that of the XRD measurements.

In the H₂-TPD profiles (Fig. 6), the position of the peak corresponds to the adsorption strength. For all these catalysts, one weak H₂ desorption peak was observed at 350 K, indicating a weak adsorption of hydrogen on the surface of metallic Ir. But when the carbon number of the alcohol increased from 1 to 3, the strength of hydrogen adsorption increased a little and then decreased when the carbon number increased. Integrating the desorption peak area, the amounts of desorbed hydrogen were obtained, which are listed in Table 4. The desorption amounts of H₂ on Ir-Re/S catalyst was 4.9 $\mu\text{mol/g}$, and this increased when the support was pretreated with alcohol. The desorption amounts of H₂ were similar for all the alcohol-pretreated SiO₂ supported catalysts. The dispersion of Ir on these catalysts, which was calculated assuming one hydrogen molecule dissociatively adsorbed on two Ir atoms, showed the same trend as the desorption amounts of H₂. The dispersion calculated by the TEM results (Table 3) was much higher than from H₂-TPD, and the amounts of exposed active metallic Ir was only approximately 32.5% of that calculated with the TEM results. This suggested that Ir might be covered by Re species because ReO_x cannot adsorb hydrogen. We calculated the moles of Ir covered by ReO_x using the results of TEM and H₂-TPD, and the data are listed in Table 4. It was found that superficial Ir atoms on the Ir-Re/S-C3 catalyst were the most covered among all the catalysts.

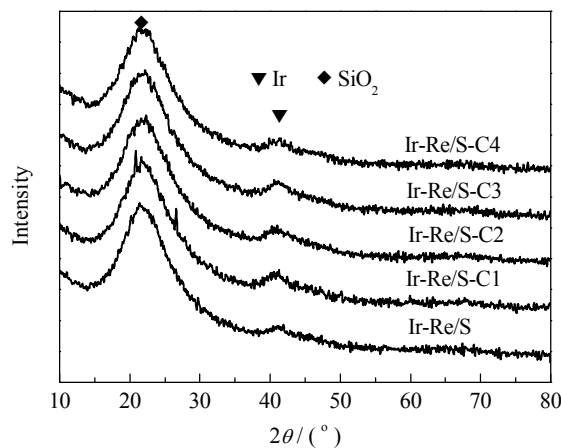


Fig. 4. XRD patterns of alcohol-pretreated SiO₂ supported catalysts after reaction.

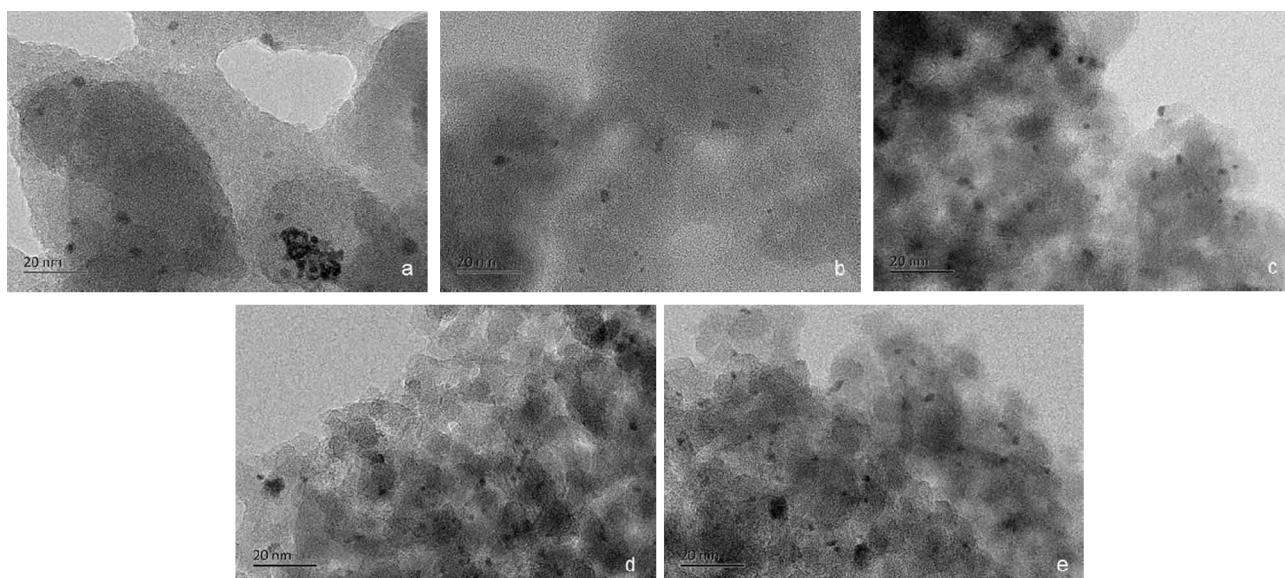


Fig. 5. HRTEM images of the spent alcohol-pretreated SiO₂ supported catalysts. (a) Ir-Re/S; (b) Ir-Re/S-C1; (c) Ir-Re/S-C2; (d) Ir-Re/S-C3; (e) Ir-Re/S-C4.

Fig. 7 shows the NH₃-TPD profiles of the alcohol-pretreated SiO₂ supported catalysts and the untreated one. A very weak NH₃ desorption peak at a wide temperature range near 573 K was detected on Ir/S. But Re/S showed one desorption peak at 490 K. All the catalysts containing Re showed a NH₃ desorption at 490 K, suggesting that the Re species was the main acidic sites. Table 5 shows the NH₃ uptake of the samples calculated by integration of the NH₃ desorption amount. All the alcohol-pretreated SiO₂ supported catalysts had a larger NH₃ up-

take amount than the untreated one, and Ir-Re/S-C3 had the highest uptake of NH₃. The NH₃ uptake indicate the amount of superficial Re species. So the alcohol-pretreated catalysts have more superficial Re species than Ir-Re/S. Therefore, it can be inferred from these results that the Re species on the alcohol-pretreated SiO₂ supported catalysts were dispersed better than on untreated one. Based on the results that most Ir atoms were covered by ReO_x and Re species particles were smaller on

Table 3

Average particle size of Ir particles of different catalysts measured by TEM.

catalyst	Average particle size of Ir species (nm)	Dispersion (%)
Ir-Re/S	3.0	36.8
Ir-Re/S-C1	2.5	44.2
Ir-Re/S-C2	2.5	44.2
Ir-Re/S-C3	2.4	46.0
Ir-Re/S-C4	2.9	38.1

Table 4

Desorption amounts of H₂ and dispersion of Ir calculated from desorbed amounts of H₂.

Catalyst	Desorption amounts of H ₂ (μmol/g)	Dispersion (%)	Ir moles covered by ReO _x (μmol/g)
Ir-Re/S	4.9	9.4	28.5
Ir-Re/S-C1	7.8	15.0	30.4
Ir-Re/S-C2	7.6	14.6	30.8
Ir-Re/S-C3	7.4	14.2	33.1
Ir-Re/S-C4	7.7	14.8	24.2

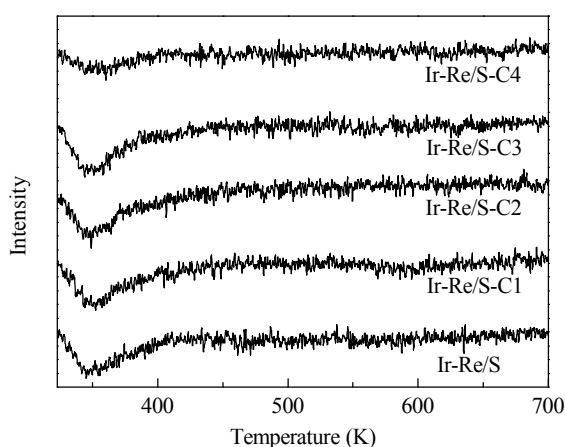


Fig. 6. H₂-TPD profiles of the alcohol-pretreated SiO₂ supported catalysts.

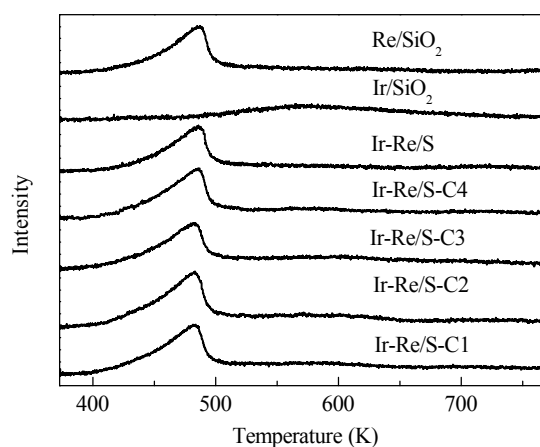


Fig. 7. NH₃-TPD profiles of the alcohol-pretreated SiO₂ supported catalysts and untreated.

Table 5
Uptake amount of NH₃ by different catalysts.

Catalyst	Uptake of NH ₃ (μmol/g)
Ir-Re/S	233.2
Ir-Re/S-C1	257.6
Ir-Re/S-C2	275.1
Ir-Re/S-C3	295.5
Ir-Re/S-C4	239.0

the alcohol-pretreated SiO₂ supported catalysts (especially for Ir-Re/S-C3 catalyst), it can be concluded that there were more Ir-ReO_x interfacial sites on the alcohol-pretreated SiO₂ supported catalysts. The Ir-ReO_x interfacial sites increased when the carbon number of the pretreatment alcohol increased from 1 to 3, and then decreased when carbon number was 4.

In order to investigate the acid types of the catalysts, FT-IR analysis of pyridine adsorption was carried out. As shown in Fig. 8, the bands at 1540 cm⁻¹ were attributed to Brønsted acidic sites and the bands at 1450 cm⁻¹ were assigned to Lewis acidic sites [35]. The absorption bands at 1490 cm⁻¹ were due to pyridine adsorption on both Brønsted acidic and Lewis acidic sites [36]. Generally, the spectra obtained when pyridine desorbed at 423, 623 and 723 K corresponded to all acidic, medium-strong acidic and strong acidic sites, respectively. This revealed that the Lewis acidic sites on the catalysts were weak acids and the Brønsted acidic sites contained weak acids and medium-strong acids. There were no strong acidic sites on the Ir-Re/S and Ir-Re/S-C3 catalysts. The B/L acidic sites ratio of the Ir-Re/S and Ir-Re/S-C3 catalysts were both approximately 3.3.

Re/S catalyst did not adsorb CO, as shown in Fig. 9. Therefore, the local environment of the Ir sites can be probed by CO adsorption using FT-IR. Adsorption of CO on Ir/S catalyst resulted in a main band at 2084 cm⁻¹. The adsorption bands shifted to lower wavenumbers on the Ir-Re system catalysts, which demonstrated that there were smaller Ir particles in the Ir-Re system catalysts and the Re species promoted the dispersion of Ir species [37].

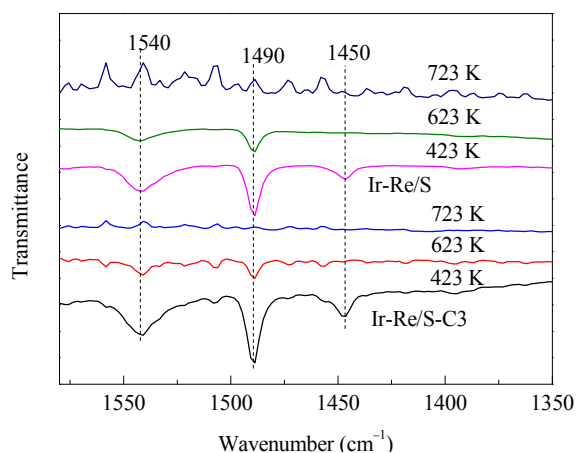


Fig. 8. FT-IR spectroscopy of pyridine adsorption on Ir-Re/S and Ir-Re/S-C3 catalysts.

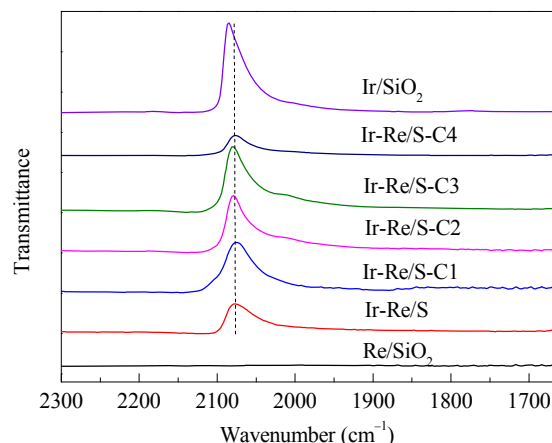


Fig. 9. Infrared spectra of adsorbed CO on different catalysts.

3.3. Catalytic activity

The catalytic performance of the alcohol-pretreated SiO₂ supported catalysts is listed in Table 6. A maximum conversion of 59.5% was achieved when the glycerol feed with the concentration of 80% reacted over Ir-Re/S-C3 at 403 K and 8 MPa. The conversion increased with an increase in carbon numbers from 1 to 3. However, there was a decrease in the conversion of glycerol when the carbon numbers of the alcohol was increased to 4. With the increase of glycerol conversion, the selectivity to 1,3-propanediol and 1,2-propanediol decreased and that to 1-propanol, 2-propanol and propane increased. This suggested that the high conversion of glycerol was accompanied by the consecutive reaction of 1,3-propanediol and 1,2-propanediol, thus leading to the lower selectivity to these and the higher selectivity to excessive decomposition byproduct. However, the ratio of removal selectivity to secondary hydroxyl groups/half of primary hydroxyl groups ($S_{2-OH}/(S_{1-OH}/2)$) of all of the catalysts varied little, which means that the pretreated SiO₂ support has little influence on $S_{2-OH}/(S_{1-OH}/2)$. All the catalysts may have the same kind of active sites. The small decrease of $S_{2-OH}/(S_{1-OH}/2)$ for the Ir-Re/S-C3 catalyst may be caused by the competitive adsorption of a higher concentration of primary hydroxyl groups. A higher removal yield of secondary hydroxyl group (Y_{2-OH}) was observed on the Ir-Re/S-C3 catalyst (28.3%). Y_{2-OH} of all the alcohol-pretreated SiO₂ supported catalysts was higher than that of the Ir-Re/S catalyst. When the weight hourly space velocity (WHSV) was increased to 0.76 h⁻¹, the performance of the Ir-Re/S-C3 catalyst is also listed in Table 6. The conversion decreased to 43.4% which was similar to Ir-Re/S. Accordingly the selectivity to 1,3-propanediol and 1,2-propanediol increased to 39.4% and 12.6%, which was also similar to that of Ir-Re/S. This coincides with the inference we proposed that the alcohol-pretreated SiO₂ supported catalysts did not promote the removal selectivity to secondary hydroxyl groups.

We also conducted an experiment on the hydrogenolysis of 1,3-propanediol over Ir-Re/S and Ir-Re/S-C3. The results are shown in Table 7. The conversion of 1,3-propanediol on Ir-Re/S-C3 was much higher than that on Ir-Re/S. In conclu-

Table 6Catalytic performance of the alcohol-pretreated SiO₂ supported catalysts^[a].

Catalyst	Conversion (%)	Selectivity (%)					C ₃ H ₈	Others ^f	S _{2-OH} /(S _{1-OH} /2) ^h	Y _{2-OH} ⁱ
		1,3-PD ^b	1,2-PD ^c	1-PO ^d	2-PO ^e					
Ir-Re/S	42.7	39.1	12.4	33.8	10.6	4.0	0.1	2.0	21.6	
Ir-Re/S-C1	53.6	35.9	11.6	37.0	10.2	5.0	0.3	2.0	26.6	
Ir-Re/S-C2	56.8	32.9	11.2	39.5	10.6	5.4	0.2	1.9	27.5	
Ir-Re/S-C3	59.5	29.4	9.1	43.1	10.6	7.4	0.4	1.8	28.3	
Ir-Re/S-C4	44.5	40.6	15.8	26.1	7.5	9.4	0.6	2.0	22.3	
Ir-Re/S-C3 ^[g]	43.8	38.8	12.4	33.9	9.4	5.1	0.4	2.1	22.2	

^a Reaction condition: $p = 8.0$ MPa, $T = 403$ K, WHSV = 0.53 h⁻¹, 1.5 g catalyst, 80 wt% glycerol aqueous solution, $V_{H_2} = 40$ mL/min, TOS = 36 h. Reduction conditions: $p = 0.1$ MPa, $V_{H_2} = 40$ mL/min, $T = 443$ K, $t = 2$ h. ^b 1,3-PD = 1,3-propanediol. ^c 1,2-PD = 1,2-propanediol. ^d 1-PO = 1-propanol. ^e 2-PO = 2-propanol. ^f Others include ethanol and ethane. ^g Reaction conditions: $p = 8.0$ MPa, $T = 403$ K, WHSV = 0.76 h⁻¹, 1.5 g catalyst, 80 wt% glycerol aqueous solution, $V_{H_2} = 40$ mL/min, $t = 36$ h. ^h Ratio of removal selectivity to secondary hydroxyl groups and half of primary hydroxyl groups. ⁱ Removal yield of secondary hydroxyl group.

sion, the conversion of glycerol over the alcohol-pretreated SiO₂ supported catalysts was increased, but there was little effect on the removal of secondary hydroxyl groups. The reverse trend of the conversion of glycerol and the selectivity to 1,3-propanediol was caused by the consecutive reaction of our target product 1,3-propanediol.

From the TEM, H₂-TPD and NH₃-TPD results, we know that there were more Ir-ReO_x interfacial sites on the alcohol-pretreated SiO₂ supported catalysts. The interfacial sites were correlated with the conversion of glycerol. This supported the suggestion that the Ir-ReO_x interfacial sites are the active sites for glycerol hydrogenolysis.

The XRD and TEM measurements of the spent catalysts revealed that the Ir particles of Ir-Re/S-C_n were smaller than Ir-Re/S, while the smallest particles was achieved on Ir-Re/S-C3. This was a result from that the interaction of metal species with isolated Si-OH promoted the formation of smaller supported metal particles [23,26,27]. Isolated Si-OH would be formed by the segregation of surface alkoxy groups [22,32,38]. Therefore, it was considered that the pretreatment of supports with alcohols increased isolated Si-OH on the support surface, resulting in the formation of smaller IrO₂ particles. It was also reported that the strong interaction between metal species and support also improved the dispersion of metal particles [24,25]. A strong interaction between IrO₂ and SiO₂ existed, which was concluded from the TPR results. This would also be a reason for the formation of smaller IrO₂ particles. Longer carbon chains of alkoxy have a better separation effect to hinder the metal precursors from aggregation, so the dispersion of Ir species and Re species increased when the carbon number of the pretreatment alcohol increased from 1 to 3. But when the

Table 7Catalytic performance in the hydrogenolysis of 1,3-propanediol over Ir-Re/S and Ir-Re/S-C3^a.

Catalyst	Conversion (%)	Selectivity (%)		
		1-PO	C ₃ H ₈	Others
Ir-Re/S	41.8	91.2	8.4	0.4
Ir-Re/S-C3	63.6	93.7	5.5	0.8

^a Reaction conditions: $p = 8.0$ MPa, $T = 403$ K, WHSV = 0.533 h⁻¹, 1.5 g catalyst, 80 wt% 1, 3-propanediol aqueous solution, $V_{H_2} = 40$ mL/min, TOS = 36 h. Reduction conditions: $p = 0.1$ MPa, $V_{H_2} = 40$ mL/min, $T = 443$ K, $t = 2$ h.

carbon number increased to 4, the amount of C4 alcohol molecules was smaller, so the dispersion of Ir species and Re species decreased. Accordingly, the conversion over Ir-Re/S-C4 decreased.

4. Conclusions

A simple method for preparing highly dispersed supported metal catalyst for glycerol hydrogenolysis was developed by the modification of a support surface using C1–C4 normal alcohols. For the catalysts prepared using the alcohol-pretreated SiO₂ supports, a higher conversion of glycerol was achieved. The higher conversion was due to more interfacial sites of Ir and ReO_x on the alcohol-pretreated SiO₂ supported catalysts. The kind of active sites on all the catalysts was similar because they gave almost the same removal selectivity to secondary alkoxy groups. A higher conversion was accompanied by a lower selectivity to 1,3-propanediol, which was caused by consecutive hydrogenolysis. However, the removal yield of secondary alkoxy groups on the alcohol-pretreated SiO₂ supported catalysts, especially Ir-Re/S-C3, was higher than that on the untreated catalyst. Therefore, by selecting an organic solvent with a suitable chain length to modify the catalyst support, the supported metal or metal oxide was adjusted or controlled to form a designed particle size and had designed surface properties. This is highly attractive for optimizing the catalytic performance of designed catalysts.

References

- [1] M. McCoy, *Chem. Eng. News*, **2006**, 84, 7.
- [2] J. Gong, F. Q. You, *ACS Sustain. Chem. Eng.*, **2015**, 3, 82–96.
- [3] Y. Nakagawa, K. Tomishige, *Catal. Sci. Technol.*, **2011**, 1, 179–190.
- [4] C. H. Zhou, J. N. Beltrami, Y. X. Fan, G. Q. Lu, *Chem. Soc. Rev.*, **2008**, 37, 527–549.
- [5] H. W. Tan, A. R. Abdul Aziz, M. K. Aroua, *Renew. Sustain. Energy Rev.*, **2013**, 27, 118–127.
- [6] O. M. Daniel, A. DeLaRiva, E. L. Kunkes, A. K. Datye, J. A. Dumesic, R. J. Davis, *ChemCatChem*, **2010**, 2, 1107–1114.
- [7] Y. Shinmi, S. Koso, T. Kubota, Y. Nakagawa, K. Tomishige, *Appl. Catal. B*, **2010**, 94, 318–326.
- [8] Y. Nakagawa, Y. Shinmi, S. Koso, K. Tomishige, *J. Catal.*, **2010**, 272, 191–194.

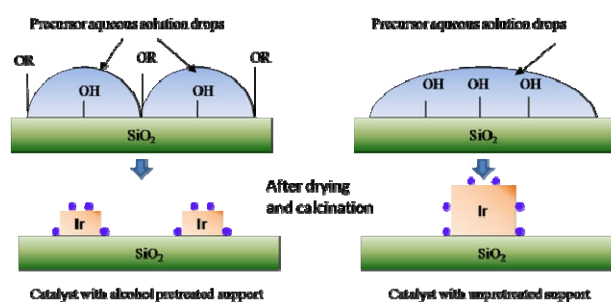
Graphical Abstract

Chin. J. Catal., 2016, 37: 2009–2017 doi: 10.1016/S1872-2067(16)62517-2

Alcohol-treated SiO₂ as the support of Ir-Re/SiO₂ catalysts for glycerol hydrogenolysis

Wenting Luo, Yuan Lyu *, Leifeng Gong, Hong Du, Miao Jiang,
Yunjie Ding *
Dalian Institute of Chemical Physics, Chinese Academy of Sciences;
University of Chinese Academy of Sciences

Alcohol pretreatment of the support promoted the formation of smaller supported metal particles and the segregation of surface alkoxy groups.



- [9] L. Ma, D. H. He, *Top. Catal.*, **2009**, 52, 834–844.
- [10] Y. M. Li, H. M. Liu, L. Ma, D. H. He, *RSC Adv.*, **2014**, 4, 5503–5512.
- [11] C. H. Deng, X. Z. Duan, J. H. Zhou, X. G. Zhou, W. K. Yuan, S. L. Scott, *Catal. Sci. Technol.*, **2015**, 5, 1540–154.
- [12] C. H. Deng, L. Leng, J. H. Zhou, X. G. Zhou, W. K. Yuan, *Chin. J. Catal.*, **2015**, 36, 1750–1758.
- [13] C. H. Deng, L. Leng, X. Z. Duan, J. H. Zhou, X. G. Zhou, W. K. Yuan, *J. Mol. Catal. A*, **2015**, 410, 81–88.
- [14] L. Leng, H. Zhang, X. Ren, J. H. Zhou, Z. J. Sui, X. G. Zhou, *J. Chem. Ind. Eng.*, **2016**, 67, 540–548.
- [15] A. Ciftci, B. X. Peng, A. Jentys, J. A. Lercher, E. J. M. Hensen, *Appl. Catal. A*, **2012**, 431–432, 113–119.
- [16] Y. Amada, Y. Shinmi, S. Koso, T. Kubota, Y. Nakagawa, K. Tomishige, *Appl. Catal. B*, **2011**, 105, 117–127.
- [17] Y. Nakagawa, X. H. Ning, Y. Amada, K. Tomishige, *Appl. Catal. A*, **2012**, 433–434, 128–134.
- [18] K. Tomishige, Y. Nakagawa, M. Tamura, *Top. Curr. Chem.*, **2014**, 353, 127–162.
- [19] Y. Nakagawa, K. Mori, K. Y. Chen, Y. Amada, M. Tamura, K. Tomishige, *Appl. Catal. A*, **2013**, 468, 418–425.
- [20] C. H. L. Tempelman, E. J. M. Hensen, *Appl. Catal. B*, **2015**, 176–177, 731–739.
- [21] M. S. Hegde, P. Bera, *Catal. Today*, **2015**, 253, 40–50.
- [22] D. H. Jiang, Y. Ding, Z. D. Pan, W. M. Chen, H. Y. Luo, *Catal. Lett.*, **2007**, 121, 241–246.
- [23] Y. Zhang, K. Hanayama, N. Tsubaki, *Catal. Commun.*, **2006**, 7, 251–254.
- [24] L. H. Shi, D. B. Li, B. Hou, Y. L. Wang, Y. H. Sun, *Fuel Process. Technol.*, **2010**, 91, 394–398.
- [25] B. T. Li, X. Y. Qian, X. J. Wang, *Int. J. Hydrogen Energy*, **2015**, 40, 8081–8092.
- [26] J. F. Chen, Y. R. Zhang, L. Tan, Y. Zhang, *Ind. Eng. Chem. Res.*, **2011**, 50, 4212–4215.
- [27] B. Wang, J. F. Chen, Y. Zhang, *RSC Adv.*, **2015**, 5, 22300–22304.
- [28] R. L. Lu, D. S. Mao, J. Yu, Q. S. Guo, *J. Ind. Eng. Chem.*, **2015**, 25, 338–343.
- [29] F. Garbassi, L. Balducci, P. Chiurlo, L. Deiana, *Appl. Surf. Sci.*, **1995**, 84, 145–151.
- [30] J. H. Z. dos Santos, P. P. Greco, F. C. Stedile, J. Dupont, *J. Mol. Catal. A*, **2000**, 154, 103–113.
- [31] Q. H. Xia, K. Hidajat, S. Kawi, *Catal. Today*, **2001**, 68, 255–262.
- [32] J. Cortes, R. Jimenez, P. Araya, *Catal. Lett.*, **2002**, 82, 255–259.
- [33] K. Baranowska, J. Okal, *Appl. Catal. A*, **2015**, 499, 158–167.
- [34] Y. V. Guryev, I. I. Ivanova, V. V. Lunin, W. Grünert, M. W. E. van den Berg, *Appl. Catal. A*, **2007**, 329, 16–21.
- [35] G. A. Eimer, S. G. Casuscelli, C. M. Chanquia, V. Elías, M. E. Crivello, E. R. Herrero, *Catal. Today*, **2008**, 133–135, 639–646.
- [36] X. P. Duan, Y. Teng, A. J. Wang, V. M. Kogan, X. Li, Y. Wang, *J. Catal.*, **2009**, 261, 232–240.
- [37] P. Bazin, O. Saur, J. C. Lavalley, M. Daturi, G. Blanchard, *Phys. Chem. Chem. Phys.*, **2005**, 7: 187–194.
- [38] S. W. Ho, Y. S. Su, *J. Catal.*, **1997**, 168, 51–59.

Page numbers refer to the contents in the print version, which include both the English version and extended Chinese abstract of the paper. The online version only has the English version. The pages with the extended Chinese abstract are only available in the print version.